European Radiology (2019) 29:2949–2957
https://doi.org/10.1007/s00330-018-5946-5

CHEST

Computed tomography improves the differentiation of infectious mediastinitis from normal postoperative changes after sternotomy in cardiac surgery

Borek Foldyna [1,2] · Martin Mueller [1] · Christian D. Etz [3] · Christian Luecke [1] · Josephina Haunschild [3] · Ines Hoffmann [4] · Matthias Gutberlet [1] · Lukas Lehmkuhl [1,5]

Received: 11 September 2018 / Revised: 2 November 2018 / Accepted: 3 December 2018 / Published online: 10 January 2019
© European Society of Radiology 2019

Abstract

Objectives To identify CT parameters independently associated with infectious mediastinitis after cardiac surgery and to improve the discrimination of patients with acute infection from those with normal postoperative changes.

Methods In this single-center, retrospective, observational cohort study, we evaluated thoracic CT scans of poststernotomy cardiac surgery patients. Inclusion criteria were clinically suspected mediastinitis, unclear CT signs (e.g., retrosternal mass), and subsequent deep revision surgery. Revision surgery and microbiological samples determined the mediastinitis status. Overall, 22 qualitative and quantitative CT imaging parameters were assessed and associated with infectious mediastinitis in univariate and multivariate regression models. Discriminative capacity and incremental value of the CT features to available clinical parameters were determined by AUC and likelihood-ratio tests, respectively.

Results Overall 105 patients (82% men; 67.0 ± 10.3 years) underwent CT and deep revision surgery. Mediastinitis was confirmed in 83/105 (79%) patients. Among available clinical parameters, only C-reactive protein (CRP) was independently associated with infectious mediastinitis (multivariate odds ratio (OR) (per standard deviation) = 2.3; $p < 0.001$). In the CT, the presence of free gas, pleural effusions, and brachiocephalic lymph node size were independently associated with mediastinitis (multivariate ORs = 1.3–6.3; $p < 0.001$–0.039). Addition of these CT parameters to CRP increased the model fit significantly ($X^2 = 17.9$; $p < 0.001$; AUC, 0.83 vs. 0.73).

Conclusion The presence of free gas, pleural effusions, and brachiocephalic lymph node size in CT is independently associated with infectious mediastinitis in poststernotomy patients with retrosternal mass. These imaging features may help to differentiate mediastinitis from normal postoperative changes beyond traditional clinical parameters such as CRP.

Key Points

- *Presence of free gas, pleural effusions, and brachiocephalic lymph node size on CT are associated independently with infectious mediastinitis.*
- *Combination of these CT parameters increases the discriminatory capacity of clinical parameters such as CRP.*

Keywords Multidetector computed tomography · Mediastinitis · Sternotomy · Cardiac surgery

Borek Foldyna and Martin Mueller contributed equally to this work.

Electronic supplementary material The online version of this article (https://doi.org/10.1007/s00330-018-5946-5) contains supplementary material, which is available to authorized users.

✉ Borek Foldyna
bfoldyna@mgh.harvard.edu

[1] Department of Diagnostic and Interventional Radiology, University of Leipzig – Heart Center, Struempellstrasse 39, 04289 Leipzig, Germany

[2] Cardiac MR PET CT Program, Massachusetts General Hospital – Harvard Medical School, Boston, MA, USA

[3] Department of Cardiac Surgery, University of Leipzig – Heart Center, Leipzig, Germany

[4] MVZ Laboratory Reising-Ackermann MD and Colleagues, Leipzig, Germany

[5] Clinic for Radiology, Cardiovascular Center Bad Neustadt, Bad Neustadt, Germany

Abbreviations

CRP C-reactive protein
HU Hounsfield unit
ICC Intra-class correlation coefficient
IQR Inter-quartile range
Ln Lymph node
OR Odds ratio
ROI Region of interest
SD Standard deviation
VOI Volume of interest

Introduction

Median sternotomy is the most common surgical approach to access the heart [1, 2]. In up to 3% of patients, median sternotomy leads to postoperative healing disorders and wound infections [3, 4] increasing the perioperative risk and costs [5–7]. Infectious mediastinitis may develop into a life-threatening condition, requiring a fast diagnosis and therapy [8, 9].

Usually, postoperative patients are monitored clinically, including visual wound control and estimation of frequently unspecific biomarkers (e.g., body temperature, C-reactive protein (CRP), and leucocytes levels). In case of suspected mediastinitis, computed tomography (CT) is often performed to confirm or reject the diagnosis. Nevertheless, most of the abnormal CT findings (e.g., retrosternal mass and free air and fluid) are common after cardiac surgery, and the final diagnosis depends on the subjective judgment of the individual examiner [10–15]. Specifically, retrosternal fluid (e.g., seroma and hematoma) is common in poststernotomy patients and may be mistakenly classified as abscesses or as mask infection signs (Fig. 1). Few more specific CT markers (e.g., pleural effusion) are based on studies performed decades ago involving old CT techniques and small cohorts [9, 16–19]. Thus, it remains unclear which image characteristics can help to distinguish mediastinitis from normal postoperative changes in contemporary cohorts using the latest equipment.

We hypothesized that a selection of qualitative and quantitative CT parameters is associated with mediastinitis and has incremental value to clinical factors for discrimination of mediastinitis from normal poststernotomy changes. Therefore, this study aimed to (1) identify CT characteristics which are independently associated with infectious mediastinitis and (2) explore their incremental value to clinical parameters.

Materials and methods

Patient population and mediastinitis definition

This single-center, retrospective, observational cohort study included poststernotomy cardiac surgery patients with clinically suspected acute infectious mediastinitis between February 2010 and October 2015. Further inclusion criteria were postoperative contrast-enhanced CT and deep revision surgery with collections of retrosternal microbiological samples. We excluded patients with exclusively superficial wound revision, and those who received revision surgery without prior imaging. We also excluded patients with imported CT images (different scan protocols) and inconclusive microbiological results or revision surgery reports (Consort diagram; supplemental Fig. 1S).

All microbiological samples were analyzed according to the national microbiology procedure quality standards [20], scoring all samples with at least one pathogen as positive. Furthermore, we searched revision surgery reports for documented intraoperative clear evidence of retrosternal infection. Following the most recent guidelines [21], patients with evidence of retrosternal infection in revision surgery or those with positive microbiological samples were rated as mediastinitis-positive. Moreover, we recorded blood levels of C-reactive protein (CRP) and leukocytes as well as the presence of diabetes mellitus prior to the revision surgery. The local ethics committee approved the study (RN: 3131-15-24082015).

CT data acquisition and scan protocol

We used a second-generation, 128-row, dual source CT scanner (Somatom Definition Flash, Siemens Healthineers) applying standard protocols. Briefly, all thorax scans were completed in cranio-caudal direction 90 s after i.v. application of 70–90 ml (flow rate, 2.5 ml/s) of nonionic iodinated contrast medium (iomeprol, 400 mg iodine/ml, Bracco Imaging). Each scan started at the thorax aperture and ended at the level of the lowest part of the lateral pleural recessus. Automatic dose modulation was applied in all cases to limit radiation exposure.

CT data evaluation

Two radiologists (BF and MM) with 5- and 1-year experience analyzed the CT data in consensus in a randomized fashion and blinded to the clinical data. All qualitative and quantitative analyses were performed using a dedicated postprocessing software (OsiriX 7.0, Pixmeo; Medical Image Processing, Analysis, and Visualization (MIPAV), Center for Information Technology, National Institutes of Health).

Qualitative analysis

The qualitative CT characteristics included the presence of free fluid, free gas, lymphadenopathy (in all mediastinal locations), skin defects, and impaired sternal condition. We also documented the presence of pericardial or pleural effusions (> 1-cm thickness) and pulmonary infiltrates, and we assessed the presence of marginal contrast enhancement in all fluid

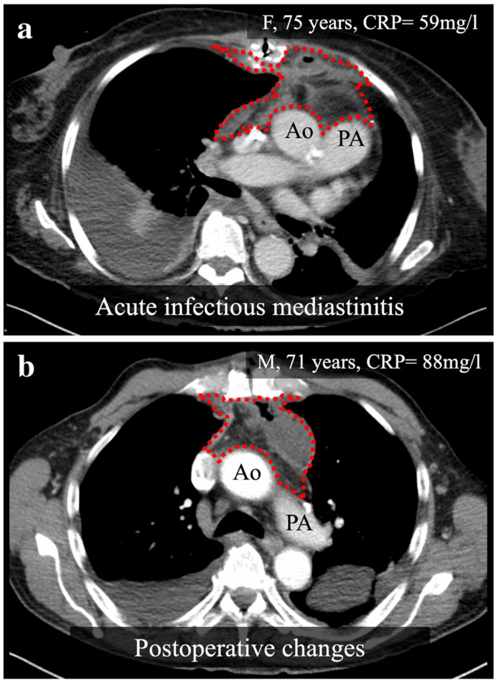

Fig. 1 Postoperative imaging findings after sternotomy. Examples of postoperative CT scans emphasizing the difficulty in differentiating between patients with mediastinal infection (**a**) and those with normal postoperative changes (**b**). Both patients presented with similar image findings in the anterior retrosternal mediastinum (red-dotted line) and elevated inflammation markers. Ao, aorta; CRP, C-reactive protein; PA, pulmonary artery

collections. In a supplemental analysis, we explored the marginal enhancement in an early (< 21 days) and in a late (≥ 21 days after initial surgery) presenting groups. The impaired sternal condition was defined as a defect/broken osteosynthesis material, presence of sternal dehiscence (> 2 mm), or osteolysis and sclerosis of sternotomy edges. Free mediastinal fluid and gas were not evaluated in case of present mediastinal drainages.

Quantitative analysis

Quantitative analysis included volume (ml) and radiodensity (Hounsfield units, HU) measurements of the retrosternal mass as well as the assessment of the maximal short-axis lymph node (Ln) size (mm), and sternal dehiscence width (mm). To measure the mediastinal volume, we segmented the retrosternal mass by interpolating multiple, consecutive, manually drawn regions of interest in transversal images. For details, see supplemental Fig. 2S. The anatomical borders for the volume segmentation were the sternum (ventral), pleura (lateral), large vessels/heart (dorsal), manubrium (cranial), and lower sterno-costal joint (caudal). We further assessed the composition of the mediastinal volume including volumes of free gas and fluid based on fixed attenuation thresholds (gas, − 1000 to − 350 HU; fluid, − 21 to + 100 HU) [22–24]. In a subset of 30 patients, volume measurements were highly reproducible, with both excellent inter- and intra-observer reliabilities (intra-class correlation coefficient (ICC) = 0.97–0.99). Each patient's mean mediastinal radiodensity was assessed using three representative ROIs.

Statistical analysis

Categorical variables were expressed as frequencies and percentages and continuous variables as medians and interquartile ranges (Q1–Q3, IQR). Continuous variables were tested for distribution using the Shapiro-Wilk test, and skewed variables were *log*-transformed. Differences between mediastinitis-positive and mediastinitis-negative patients were tested with the independent Student *t* test, Mann-Whitney *U* test, or Fisher exact test as appropriate.

In univariate logistic regressions, we associated individual CT parameters with mediastinitis and used multivariate conditional backward selection to render independent parameters from those which reached significance ($p < 0.05$) in the univariate analysis. Collinearity was excluded by calculating the variance inflation factor which was in average 1.02 (collinearity threshold = 4). We used receiver operator characteristic (ROC) curves to determine the area under the curve (AUC) as a measure of discriminatory capacity for mediastinitis in following models: (1) clinical parameters, (2) CT parameters, and (3) combination of CT + clinical parameters (nested model). The DeLong method was applied to test the difference of discriminatory capacity between the clinical and CT parameters (nonnested models). To test the incremental value of CT to the clinical parameters, we evaluated whether the model fit increases by adding CT parameters to the clinical parameters using the likelihood-ratio test (nested model). Corresponding equations to calculate individual risk are provided in the supplemental Text 1S. We used STATA 14.0 for all the analyses and considered two-sided p value of < 0.05 as statistically significant without adjustment for multiple comparisons.

Results

Patient characteristics and clinical parameters

The study population consisted of 105 patients, 86 (81.9%) males with a median age of 68.0 (62.0–74.0) years (Table 1). The interval between the initial surgery and CT was 22.0 (12.0–35.5) days followed by the revision surgery in median 1.0 (1.0–3.0) day later. Infectious mediastinitis was detected in 83/105 (79.1%) patients with *Staphylococcus epidermidis* as the most frequent pathogen (31.4%) (supplemental Table 2S). All qualitative CT parameters, lymph node diameters, and sternum dehiscence width were assessed in all 105 patients while the measurement of volume and density was available in 99/105 (94.3%) patients. The six individuals were excluded

Table 1 Clinical patient characteristics

Clinical characteristic	All patients ($n = 105$)	Mediastinitis yes ($n = 83$)	Mediastinitis no ($n = 22$)	p
Age (years)	68.0 (62.0–74.0)	70.0 (63.0–75.0)	66.5 (54.3–71.3)	0.084
Male, n (%)	86 (81.9)	67 (80.7)	19 (86.4)	0.757
Height (cm)	173.5 (167.8–178.3)	173.5 (167.8–178.0)	174.0 (167.5–179.8)	0.948
Weight (kg)	86.0 (76.4–97.5)	86.0 (78.1–96.0)	91.0 (73.9–103.0)	0.288
BMI (kg/m^2)	29.5 (26.0–32.8)	29.5 (26.1–32.5)	29.3 (24.9–36.3)	0.544
Interval surgery to CT (days)	22.0 (12.0–35.5)	22.0 (12.0–35.0)	24.5 (12.8–111.0)	0.395
Concomitant diseases, n (%)				
Arterial hypertension	92 (87.6)	72 (86.7)	20 (90.9)	0.732
Hyperlipidemia	62 (59.0)	51 (61.4)	11 (50.0)	0.332
Diabetes mellitus	54 (51.4)	47 (56.6)	7 (31.8)	0.038
Renal insufficiency	18 (17.1)	17 (20.5)	1 (4.5)	0.112
Current smoker	15 (14.3)	14 (16.9)	1 (4.5)	0.185
COPD	14 (13.3)	12 (14.5)	2 (9.1)	0.729
Pulmonary hypertension	15 (14.3)	14 (16.9)	1 (4.5)	0.185
PAD	12 (11.4)	11 (13.3)	1 (4.5)	0.453
Medication, n (%)				
Anticoagulation	97 (92.4)	75 (90.4)	22 (100.0)	1.000
Immunosuppression	4 (3.8)	4 (4.8)	0 (0.0)	–
Serum biomarkers				
CRP (mg/l)	128.4 (65.0–222.9)	136.9 (82.0–229.0)	65.0 (7.8–128.2)	0.001
Leucocytes (Gpt/l)	10.1 (8.0–13.5)	10.6 (8.0–14.1)	9.3 (8.0–11.6)	0.204

Patient characteristics stratified by the presence of infectious mediastinitis. Continuous variables are listed as median (IQR). *Ao* aorta, *BMI* body mass index, *COPD* chronic obstructive pulmonary disease, *CRP* C-reactive protein, *PAD* peripheral arterial disease

from the quantitative analysis due to insufficient image quality (i.e., hardening artifacts due to implants $n = 3$ or high image noise $n = 3$). One had normal postoperative changes while the remaining five had mediastinitis.

Clinical parameters

Among the clinical parameters, CRP was higher, and diabetes mellitus was more common in patients with mediastinitis (Table 1). In the multivariate analysis, exclusively the CRP was independently associated with mediastinitis (OR (per SD) = 2.3; 95% CI, 1.38–3.69; $p = 0.001$) (supplemental Table 3S). The majority of the patients (65%) underwent coronary bypass, valvular surgery (38%), or replacement of the aorta (12%).

CT characteristics

While free mediastinal fluid was present in all patients, the prevalence of other CT parameters ranged between 11.0 and 69.8%. Free gas and pleural effusions were nearly twice as common in patients with mediastinitis compared to those with normal postoperative changes (Table 2). The univariate regression analysis has confirmed these findings, and the multivariate regression has revealed independent associations of free gas and pleural effusions with mediastinitis (free gas: OR = 3.9, 95% CI 1.27–11.78, $p = 0.017$; pleural effusion: OR = 6.3, 95% CI 2.06–19.10, $p = 0.001$) (Table 3). The presence of fluid margin enhancement was not associated with mediastinitis. There was also no association in a subanalysis stratified by the time point of the CT relative to the initial surgery (< 21 vs. ≥ 21 days) (supplemental Table 4S).

Regarding the quantitative measures, the volume of free retrosternal fluid was significantly higher in patients with mediastinitis compared to those with normal postoperative changes (112.2 (89.7–139.3) vs. 85.2 (63.8–106.5) ml, $p = 0.009$). While the volume was associated with mediastinitis in the univariate analysis (OR (per 10 ml increase) = 1.1; 95% CI, 1.01–1.29; $p = 0.030$), the significance vanished after adjustment for other CT parameters ($p = 0.339$). The median volume of free air was low (0.03 (0.01–0.19 ml)) but ranged between 0 and 107.1 ml. Even though the median volume of free air was higher in patients with mediastinitis compared to those without (0.06 vs. 0.01 ml, $p = 0.013$) (Table 2), it was not significantly associated with mediastinitis ($p = 0.411$) in the univariate regression (Table 3). The overall median radiodensity of retrosternal mass did not differ between patients with and without mediastinitis ($p = 0.231$) (Tables 2 and 3).

Table 2 CT characteristics stratified by mediastinitis status

CT characteristic	All patients ($n = 105$)	Mediastinitis yes ($n = 83$)	Mediastinitis no ($n = 22$)	p
Qualitative				
Free fluid	105 (100.0)	83 (100.0)	22 (100.0)	–
Margin enhancement	59 (55.7)	50 (61.0)	9 (40.9)	0.145
Free gas	73 (69.5)	63 (75.9)	10 (45.5)	0.009
Lymphadenopathy	36 (34.3)	31 (37.4)	5 (22.7)	0.312
Pericardial effusion	36 (34.3)	28 (33.7)	8 (36.4)	1.000
Pleural effusion	74 (70.5)	65 (78.3)	9 (40.9)	0.001
Pulmonary infiltrates	12 (11.4)	10 (9.1)	2 (12.1)	1.000
Sternum status				
Dehiscence	70 (66.7)	56 (67.5)	14 (63.6)	0.801
Lysis	31 (29.5)	26 (31.3)	5 (22.7)	0.600
Sclerosis	21 (20.0)	16 (19.3)	5 (22.7)	0.767
Broken cerclages	42 (40.0)	33 (39.8)	9 (40.9)	1.000
Skin defect	40 (38.1)	35 (42.2)	5 (22.7)	0.138
Quantitative				
Total volume (ml)	250.4 (195.8–311.3)	261.5 (201.3–322.7)	231.5 (138.4–265.7)	0.078
Air (ml)	0.03 (0.01–0.19)	0.06 (0.01–0.21)	0.01 (0.004–0.08)	0.014
Fluid (ml)	106.5 (83.5–139.0)	112.2 (89.7–139.3)	85.2 (63.8–106.5)	0.009
Radiodensity (HU)	−3.8 (−15.2–6.6)	−3.6 (−13.3–7.3)	−12.1 (−26.0–5.1)	0.231
Lymph node sizes (mm)				
Parasternal	2.0 (0.0–4.0)	2.0 (0.0–4.0)	3.0 (2.0–4.0)	0.182
Brachiocephalic	5.0 (3.0–7.0)	5.0 (3.0–7.0)	4.0 (2.0–5.0)	0.024
Anterior mediastinal	5.0 (4.0–6.0)	5.0 (4.0–7.0)	5.0 (4.0–6.0)	0.858
Posterior mediastinal	8.0 (6.0–11.0)	9.0 (6.0–9.0)	7.5 (6.0–11.0)	0.229
Sternum dehiscence (mm)	5.0 (0.0–12.0)	5.0 (0.0–12.0)	5.5 (0.0–14.0)	0.736

CT computed tomography, *HU* Hounsfield units

Among the 83 patients with mediastinitis, only 5/83 (6%) presented with lymphadenopathy (i.e., Ln size > 10 mm at any location). Although not reaching the threshold of 10 mm, the brachiocephalic lymph nodes were larger in patients with mediastinitis compared to those with normal postoperative changes (median 5.0 (3.0–7.0) vs. 4.0 (2.0–5.0) mm, $p = 0.024$). The size of the lymph nodes in other locations did not differ significantly. Although the difference of the median size was small, the size of brachiocephalic Ln revealed a significant univariate association with mediastinitis (OR (per mm increase) = 1.3; 95% CI, 1.01–1.65; $p = 0.014$). Moreover, this association was independent of other CT parameters in the multivariate regression (adjusted OR = 1.3; 95% CI, 1.01–1.65; $p = 0.039$) (Table 3).

Incremental value of the CT to CRP

In the ROC analysis, the independent CT parameters reached a good discriminatory capacity (AUC = 0.81; 95% CI, 0.70–0.92), which was comparable to the one of the CRP (AUC = 0.73; 95% CI, 0.59–0.86) (DeLong test for the difference, $p = 0.337$). Adding the CT parameters to CRP (nested model) resulted in a statistically significant improvement of model fit (likelihood-ratio test (3 degrees of freedom): $X^2 = 17.9$; $p < 0.001$) and AUC of 0.83 (95% CI, 0.72–0.94) (Fig. 2).

Discussion

Our study of CT findings in poststernotomy patients with suspected mediastinitis and retrosternal mass on CT has two major findings. First, the presence of free gas, pleural effusion, and the brachiocephalic Ln size are independent imaging markers of deep mediastinal infection. Second, addition of these markers to CRP increases the discriminatory capacity of CRP significantly. Taken as a whole, our findings provide a selection of independent CT parameters which may help with the challenging discrimination of infectious mediastinitis from normal postoperative changes.

Even though the CT has already been routinely used to confirm or reject clinically suspected mediastinitis, it is unknown which CT characteristics can discriminate between mediastinitis and normal mediastinal changes after cardiac surgery. Older studies have described a high sensitivity and low

Table 3 Independent associations of selected CT features with mediastinitis

CT parameters	Univariate			Multivariate—all with $p > 0.05$ in univariate			Multivariate—backward selected independent var.		
	OR	95% CI	*p*	OR	95% CI	*p*	OR	95% CI	*p*
Qualitative									
Free fluid	–	–	–						
Margin enhancement	2.3	0.87–5.89	0.096						
Free gas	3.8	1.42–10.06	0.008	4.7	1.46–15.24	0.009	3.9	1.27–11.78	0.017
Lymphadenopathy	2.0	0.67–5.92	0.217						
Pericardial effusion	0.9	0.35–2.45	0.872						
Pleural effusion	4.9	1.83–13.32	0.002	5.4	1.55–18.54	0.008	6.3	2.06–19.10	0.001
Pulmonary infiltrates	1.4	0.27–6.67	0.712						
Sternum status									
Dehiscence	1.2	0.45–3.22	0.708						
Lysis	1.6	0.50–5.00	0.436						
Sclerosis	0.9	0.28–3.09	0.914						
Broken cerclages	0.9	0.36–2.40	0.890						
Skin defect	2.4	0.82–7.20	0.110						
Quantitative									
Total volume (ml)	1.0	0.99–1.01	0.207						
Air (ml)	1.4	0.64–2.95	0.411						
Fluid (ml)	1.01	1.00–1.03	0.030	1.0	0.99–1.02	0.339			
Radiodensity (HU)	1.0	1.00–1.05	0.124						
Lymph node sizes (mm)									
Parasternal	0.9	0.79–1.09	0.369						
Brachiocephalic	1.3	1.06–1.62	0.014	1.3	1.00–1.65	0.050	1.3	1.01–1.65	0.039
Anterior mediastinal	1.0	0.83–1.19	0.928						
Posterior mediastinal	1.1	0.94–1.27	0.250						
Sternum dehiscence (mm)	1.0	0.91–1.04	0.417						

CI confidence interval, *CT* computed tomography, *HU* Hounsfield units, *OR* odds ratio

specificity of various CT qualitative characteristics, mainly pointing out the presence of free fluid and gas as potential markers [10–15]. However, all these studies focused on the qualitative assessment without accounting for quantitative measures (e.g., fluid/gas volume, radiodensity, and lymph node size) and lacked power due to a low number of patients with confirmed infections. Thus, there was a need for an investigation in a large contemporary cohort with a high enough prevalence of confirmed infections, using state-of-the-art scanner technology and involving qualitative and quantitative CT parameters. Our study delivers this data and employs qualitative and quantitative CT findings in combination with clinical parameters in a cohort with high prevalence of mediastinitis.

The current investigation confirms the low specificity in the majority of the 22 tested CT parameters as in part reported in the past. For example, all patients presented with retrosternal mass, which is in agreement with previous reports describing imaging findings after sternotomy [10, 12–14]. The high prevalence and low specificity limit the diagnostic value of qualitative imaging markers if considering only their presence. Thus, to optimally leverage the information provided by the CT image, we assessed the volume and radiodensity of the retrosternal mass. Indeed, the volume of free fluid within the retrosternal mass was associated with mediastinitis, although its presence was not decisive while found in the entire study population.

The volume of free air within the retrosternal mass was low (median 0.03 ml) and not associated with mediastinitis. However, patients with free air in the retrosternal location had almost four times higher likelihood to have mediastinitis (OR = 3.9) compared to those with retrosternal mass without free air.

Furthermore, we added measurements of lymph node diameters to enhance the clinical standard of reporting the sole presence of regional lymphadenopathy. Even though the presence of lymphadenopathy (i.e., at least one lymph node > 10 mm) was not associated with mediastinitis, the measurement of Ln sizes in separate locations revealed that the exclusively increase of brachiocephalic Ln size was significantly

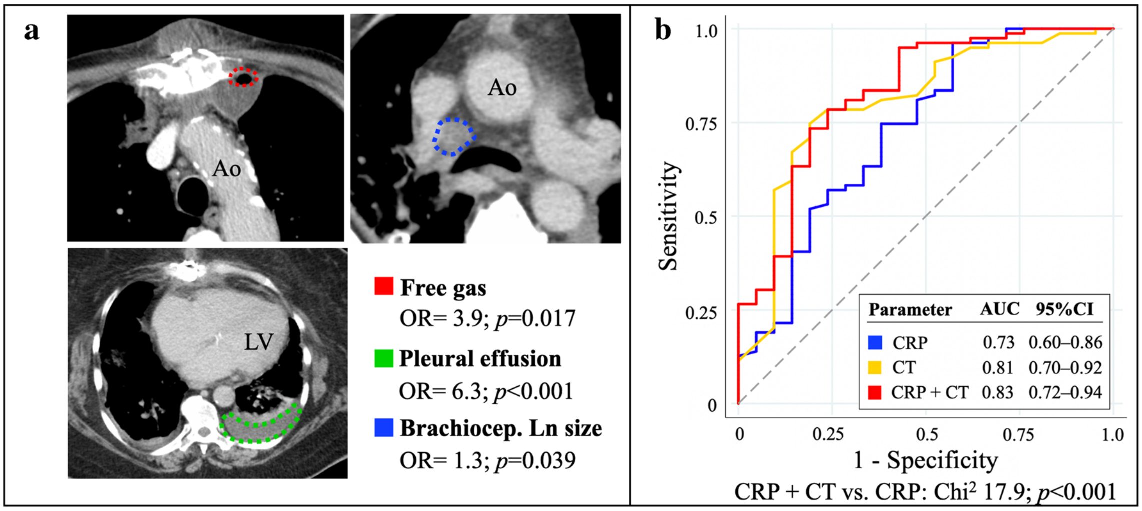

Fig. 2 Discriminatory capacity of the CT features and CRP. **a** The three selected CT features independently associated with infectious mediastinitis (free gas, pleural effusion, and brachiocephalic lymph node size) with corresponding multivariate odds ratios. **b** The discriminatory capacity of CT features, CRP, and the combination of both with the likelihood-ratio test results indicating an improvement of the model fit by adding CT to CRP. Ao, aorta; AUC, area under the curve; CRP, C-reactive protein; CT, computed tomography; LV, left ventricle; OR, odds ratio (multivariate)

associated with acute mediastinal infection. Thus, we assume that considering the Ln location and alternatively lower thresholds may be superior to the routinely used general approach and threshold of 10 mm. The brachiocephalic Ln size exceeded 10 mm in only 6% (5/83) of the mediastinitis-positive patients; thus, the majority would not have fulfilled the lymphadenopathy criteria. The specific enlargement of brachiocephalic Ln may be explained by the predominant drainage of anterior mediastinum including the thymus, thyroid glands, heart, and pericardium [25].

The observation that pleural effusions had over six times higher probability of mediastinitis confirms an old small case-control study ($n = 21$) showing that bilateral pleural effusions combined with a mediastinal mass may be an indicator for poststernotomy infection [13]. Besides confirming these findings in a larger group of patients, we show that pleural effusion represents a marker which is independent of other CT parameters. These findings encourage future studies to investigate the pathophysiology of pleural effusions in mediastinitis.

Interestingly, neither the presence of marginal enhancement nor the overall radiodensity of the retrosternal mass was associated with mediastinitis. These results are somewhat contrary to a study which has suggested that margin enhancement may be a marker of mediastinitis at least 14 days after the initial surgery [11]. However, this conclusion is based on an observation of one single postoperative patient (9th postoperative day) with a proven infection and missing enhancement. In a stratified analysis (< 21 vs. ≥ 21 days after initial surgery), there was no diagnostic value of margin enhancement or density increase in those with a longer interval between initial surgery and CT imaging. According to other studies, marginal enhancement in the CT has been described in numerous pathological conditions (septic and aseptic) including acute pancreatitis [26], acute descending necrotizing mediastinitis [11], and pericarditis [27]. Thus, we conclude that marginal enhancement may indicate inflammation rather than infection. Moreover, our results question the use of contrast agents in patients after cardiac surgery and encourage future studies to investigate the benefits of contrast agents in postoperative patients. In the future, more sophisticated techniques, such as the positron emission tomography with 2-deoxy-2-[fluorine-18]fluoro-D-glucose integrated with CT (^{18}FDG-PET/CT), may be a helpful tool to distinguish between infection and aseptic inflammation by delivering additional metabolic data [28].

The CRP, an independent marker of mediastinitis, presented with a moderate discriminatory capacity (AUC, 0.73). Therefore, clinical parameters may benefit from additional imaging features as shown by the increased model fit after adding CT parameters to CRP. Furthermore, looking at the shape of the AUC curves, apparently, the difference in AUC between CT and CRP + CT is caused by the high specificity/low sensitivity and high sensitivity/low specificity areas at the borders of the AUC curves. On the other hand, at the point with both optimal sensitivity and specificity, the values hardly differ, indicating that CRP could even be ignored.

Our study has limitations. The number of cases is too low for a complete inclusion of all potential imaging and clinical confounders. However, it is larger than the previously evaluated cohorts, and it is the first study performing adjustment for potential confounders. Advanced clinical measures of infection were not available in all patients; thus, we relied on the traditional ones (i.e., CRP and leukocyte counts). Studies incorporating further clinical measures of infection/sepsis are warranted. Finally, the patient selection in our study (revision surgery and CT) may have introduced a selection bias reducing the generalizability of our results. However, particular patients with unclear CT findings, as included in our study, are the most challenging ones and may benefit from the presented results the most. Our study is of exploratory nature, and future prospective studies need to validate our results and should investigate the potential positive influence on the survival after cardiac surgery.

Conclusion

The presence of free gas, pleural effusions, and brachiocephalic lymph node size in CT is independently associated with infectious mediastinitis in poststernotomy patients with retrosternal mass. After validation in future studies, these imaging features may help to differentiate mediastinitis from normal postoperative changes beyond traditional clinical parameters such as CRP.

Acknowledgments BF received unrelated funding from the German Research Foundation (DFG) project 290004377 (FO 993/1).

Funding The authors state that this work has not received any funding.

Compliance with ethical standards

Guarantor The scientific guarantor of this publication is Prof. Dr. Matthias Gutberlet.

Conflict of interest The authors of this manuscript declare no relationships with any companies, whose products or services may be related to the subject matter of the article.

Statistics and biometry One of the authors has significant statistical expertise. No complex statistical methods were necessary for this paper.

Informed consent Written informed consent was waived by the Institutional Review Board.

Ethical approval Institutional Review Board approval was obtained.

Methodology
• retrospective
• observational
• performed at one institution

Publisher's Note Springer Nature remains neutral with regard to jurisdictional claims in published maps and institutional affiliations.

References

1. Barsoum EA, Azab B, Shah N et al (2015) Long-term mortality in minimally invasive compared with sternotomy coronary artery bypass surgery in the geriatric population (75 years and older patients). Eur J Cardiothorac Surg 47:862–867. https://doi.org/10.1093/ejcts/ezu267
2. Brown ML, McKellar SH, Sundt TM, Schaff HV (2009) Ministernotomy versus conventional sternotomy for aortic valve replacement: a systematic review and meta-analysis. J Thorac Cardiovasc Surg 137:670–679.e5. https://doi.org/10.1016/j.jtcvs.2008.08.010
3. Buja A, Zampieron A, Cavalet S et al (2012) An update review on risk factors and scales for prediction of deep sternal wound infections. Int Wound J 9:372–386. https://doi.org/10.1111/j.1742-481X.2011.00896.x
4. Gorlitzer M, Wagner F, Pfeiffer S et al (2013) Prevention of sternal wound complications after sternotomy: results of a large prospective randomized multicentre trial. Interact Cardiovasc Thorac Surg 17:515–522. https://doi.org/10.1093/icvts/ivt240
5. Brown PP, Kugelmass AD, Cohen DJ et al (2008) The frequency and cost of complications associated with coronary artery bypass grafting surgery: results from the United States Medicare Program. Ann Thorac Surg 85:1980–1986. https://doi.org/10.1016/j.athoracsur.2008.01.053
6. Speir AM, Kasirajan V, Barnett SD, Fonner E (2009) Additive costs of postoperative complications for isolated coronary artery bypass grafting patients in Virginia. Ann Thorac Surg 88:40–46. https://doi.org/10.1016/j.athoracsur.2009.03.076
7. Chan M, Yusuf E, Giulieri S et al (2016) A retrospective study of deep sternal wound infections: clinical and microbiological characteristics, treatment, and risk factors for complications. Diagn Microbiol Infect Dis 84:261–265. https://doi.org/10.1016/j.diagmicrobio.2015.11.011
8. Athanassiadi KA (2009) Infections of the mediastinum. Thorac Surg Clin 19:37–45. https://doi.org/10.1016/j.thorsurg.2008.09.012
9. van Wingerden JJ, Maas M, Braam RL, de Mol BA (2016) Diagnosing poststernotomy mediastinitis in the ED. Am J Emerg Med 34:618–622. https://doi.org/10.1016/j.ajem.2015.12.048
10. Bitkover CY, Cederlund K, Aberg B, Vaage J (1999) Computed tomography of the sternum and mediastinum after median sternotomy. Ann Thorac Surg 68:858–863. https://doi.org/10.1016/S0003-4975(99)00549-4
11. Exarhos DN, Malagari K, Tsatalou EG et al (2005) Acute mediastinitis: spectrum of computed tomography findings. Eur Radiol 15:1569–1574. https://doi.org/10.1007/s00330-004-2538-3
12. Jolles H, Henry DA, Roberson JP, Cole TJ, Spratt JA (1996) Mediastinitis following median sternotomy: CT findings. Radiology 201:463–466. https://doi.org/10.1148/radiology.201.2.8888241
13. Misawa Y, Fuse K, Hasegawa T (1998) Infectious mediastinitis after cardiac operations: computed tomographic findings. Ann Thorac Surg 65:622–624
14. Yamaguchi H, Yamauchi H, Yamada T, Ariyoshi T, Aikawa H, Kato Y(2001) Diagnostic validity of computed tomography for mediastinitis after cardiac surgery. Ann Thorac Cardiovasc Surg 7:94–98
15. Yamashiro T, Kamiya H, Murayama S et al (2008) Infectious mediastinitis after cardiovascular surgery: role of computed tomography. Radiat Med 26:343–347. https://doi.org/10.1007/s11604-008-0238-7
16. Breatnach E, Nath PH, Delany DJ (1986) The role of computed tomography in acute and subacute mediastinitis. Clin Radiol 37:139–145. https://doi.org/10.1016/S0009-9260(86)80383-X
17. Carrol CL, Jeffrey RB Jr, Federle MP, Vernacchia FS (1987) CT evaluation of mediastinal infections. J Comput Assist Tomogr 11:449–454
18. Elia S, End A, Canalis E, Lode H, Granai Vittoria A, Petrella G (2013) Mediastinitis: causes, management and outcomes. In: Rohde

G, Subotic D (eds) Complex pleuropulmonary infections. European Respiratory Society, Norwich, UK, pp 122–140
19. Kay HR, Goodman LR, Teplick SK, Mundth ED (1983) Use of computed tomography to assess mediastinal complications after median sternotomy. Ann Thorac Surg 36:706–714
20. Herrmann M, Kniehl E, Mauch H, Podbielski A (2007) MiQ: Qualitätsstandards in der mikrobiologisch-infektiologischen Diagnostik, MiQ Grundwerk Heft 1–29. Urban & Fischer, Munich
21. Horan TC, Andrus M, Dudeck MA (2008) CDC/NHSN surveillance definition of health care–associated infection and criteria for specific types of infections in the acute care setting. Am J Infect Control 36:309–332. https://doi.org/10.1016/j.ajic.2008.03.002
22. Abramowitz Y, Simanovsky N, Goldstein MS, Hiller N (2009) Pleural effusion: characterization with CT attenuation values and CT appearance. AJR Am J Roentgenol 192:618–623. https://doi.org/10.2214/AJR.08.1286
23. Kim SH, Chung JH, Kwon BJ, Song SW, Choi WS (2014) The associations of epicardial adipose tissue with coronary artery disease and coronary atherosclerosis. Int Heart J 55:197–203
24. McWilliams SR, O'Connor OJ, McGarrigle AM et al (2012) CT-based estimation of intracavitary gas volumes using threshold-based segmentation: in vitro study to determine the optimal threshold range: gas volume estimation with CT. J Med Imaging Radiat Oncol 56:289–294. https://doi.org/10.1111/j.1754-9485.2012.02375.x
25. Riquet M, Le Pimpec-Barthes F, Hidden G (2001) Lymphatic drainage of the pericardium to the mediastinal lymph nodes. Surg Radiol Anat 23:317–319. https://doi.org/10.1007/s00276-001-0317-2
26. Balthazar EJ, Robinson DL, Megibow AJ, Ranson JH (1990) Acute pancreatitis: value of CT in establishing prognosis. Radiology 174:331–336. https://doi.org/10.1148/radiology.174.2.2296641
27. Klein AL, Abbara S, Agler DA et al (2013) American Society of Echocardiography clinical recommendations for multimodality cardiovascular imaging of patients with pericardial disease: endorsed by the Society for Cardiovascular Magnetic Resonance and Society of Cardiovascular Computed Tomography. J Am Soc Echocardiogr 26:965–1012.e15. https://doi.org/10.1016/j.echo.2013.06.023
28. Vaidyanathan S, Patel CN, Scarsbrook AF, Chowdhury FU (2015) FDG PET/CT in infection and inflammation—current and emerging clinical applications. Clin Radiol 70:787–800. https://doi.org/10.1016/j.crad.2015.03.010